Simulation of a stand-alone renewable hydrogen system for residential supply
Simulación de un sistema autónomo de hidrógeno renovable para uso residencial

Martín Hervello [a], Víctor Alfonsín [b], Ángel Sánchez [c], Ángeles Cancela [d] & Guillermo Rey [e]

[a] PhD Universidad de Vigo, España. hervello@hotmail.com
[b] PhD Student., Centro Universitario de la Defensa de Marín, España, valfonsin@cud.uvigo.es
[c] PhD Universidad de Vigo, España., asanchez@uvigo.es
[d] PhD Universidad de Vigo, España, chiqui@uvigo.es
[e] PhD Student., Centro Universitario de la Defensa de Marín, España, guillermo.rey@cud.uvigo.es

Abstract
Computer simulation is a first logical step before taking a project to physical construction beside it is a powerful tool in energy network design. Combined systems are used to improve availability for energy supplied by renewable systems. The main inconvenient of some renewable energy sources is their highly seasonal nature, with great variations over time that can impede their use as the basis for consumption and limits them to peak demand times. The aim of this work is to simulate to verify the energetic sufficiency of a family house with renewable energies (wind, solar-photovoltaic) using a hybrid system of batteries and hydrogen. For that, Simulink®-Matlab® program was used considering meteorological data provided by CINAM (Galician Center for Environmental Research and Information). The model can be applied to determine the feasibility of implementing an energy network in specific places, and to predict energy flows and system behavior throughout the year.

Keywords: Hybrid, hydrogen, renewable energy, energy storage, simulation, modeling.

Resumen
La simulación por ordenador es un primer paso lógico previo a la realización de un proyecto de una construcción física además de ser una herramienta para el diseño de redes de energía. Los sistemas combinados son una solución para mejorar la disponibilidad de la energía suministrada con medios renovables. El principal inconveniente de las fuentes de energías renovables es su naturaleza altamente estacional, con grandes variaciones en el tiempo que pueden impedir el uso como base de consumo y limitar las horas de máxima demanda. El objetivo de este trabajo es realizar simulaciones para comprobar la autosuficiencia energética de una vivienda unifamiliar en base a energías renovables (eólica, solar-fotovoltaica) utilizando como medio de almacenamiento un sistema híbrido de baterías e hidrógeno. Para ello se ha utilizado el programa Simulink®-Matlab® teniendo en cuenta los datos meteorológicos proporcionados por METEO-Galicia. El modelo puede ser aplicado para determinar la viabilidad de implementar una red energética en regiones específicas, y predecir el flujo de energía y el comportamiento del sistema durante todo el año.

Palabras clave: Híbrido; hidrógeno, energía renovable, almacenamiento de energía, simulación, modelado.

1. Introduction

Against a background of increasingly expensive fossil fuels [1], due to constantly growing worldwide demand, and the environmental risks those fuels inherently bear, such is a rising greenhouse gas emissions [2], a steady but generalized use of renewable energies can be noted, often encouraged by institutional policy [3,4].

Their use is now not only contemplated for sporadic supply of small electrical systems, but has opened up to include a wide range of possibilities such as: electricity supply to places where main grid does not cover [5,6];

vehicles [7,8]; combined use with the electricity grid [9,10]; or with predominant energy supply systems [11]. All these alternatives are centered on a common axis of on-site hydrogen production. For this reason, when implementing an energy structure including renewable energies, the knowledge of meteorological data for specific areas is very important, because the geographic factor has of great importance [12,13] in order to evaluate the potential of energy, and to make appropriate configuration choices.

The main disadvantage of some renewable energy sources is their seasonal nature, which means great variability over time, not forgetting that, besides this

seasonal effect, solar energy must also take into consideration the number of daylight hours [14,15]. These factors make it difficult to use such sources as a basis for consumption and limits them to peak use times, leading to a waste of great quantities of clean and cheap energy in places where it cannot be fed into the grid.

Due to photovoltaic and wind energies can become complementary to some extent, these have been chosen for this proposal.

In this paper a model of a small wind generator combined with a number of photovoltaic panels to meet a standard system needs is presented. Energy generated is managed by a control system that distributes it according to the situation and needs of the system.

2. Model description

Dynamic simulation of complex systems is a powerful design and analysis tool, with the subsequent saving in time and money as the step from theory to practice is considerably eased and the construction of physical prototypes is made less expensive once a close approximation to real behavior is known. In this case the Simulink® package from Matlab® has been used for modeling purposes.

In this model, energy obtained from the wind generator and several photovoltaic panels is simulated. There are three possible routes for this energy: the first is directly to satisfy demand; the second, store it in a battery before using; and

the third, and most complex, to feed an electrolyzer to convert electric excess into hydrogen [16], which is sent to a buffer that, once full, activates a compressor to send it to a storage tank where it can be converted back to energy in a fuel cell when required. Fig. 1 shows a general diagram of the model, in which energy flows are in red and hydrogen flows in blue.

Due to meteorological data are provided every 10 minutes (which is more than acceptable as a frequency for annual studies), the individual units will be simulated in steady state (as it would not make sense to waste calculation time when the time interval is greater in range than the dynamics of any of the process units), and then the whole system will be simulated dynamically.

All the power generation and consumption units are connected to a DC bus, by means of power converters, except in the case of the battery, connected directly, to provide an approximate voltage of 48 V to the bus. These units are needed to condition the voltage from the various elements to the bus; we assume efficiency at 95% for all the DC-DC converters, and at 92% for the DC-AC ones. The control for the energy flows from all of these units operates according to the energy arriving in the system and the system state.

2.1. Meteorological Data and Household Demand

The location chosen for this simulation is Marco da Curra, located in the Monferro council district which is on the northwest of the Iberian Peninsula (Latitude: 43.34º, Longitude -7.89, Altitude: 651 m), and for which 2006 was chosen as a typical meteorological year.

Data were provided by CINAM (Galician Centre for Environmental Research and Information). [17] Fig. 2a and 2b show solar radiation and wind speed throughout the year, respectively. It can be seen that energy production from the two systems is somewhat complementary, as solar production from the photovoltaic panels during the middle months of the year subsides at the start and end of the year, but at year's end when the increase in stronger air currents
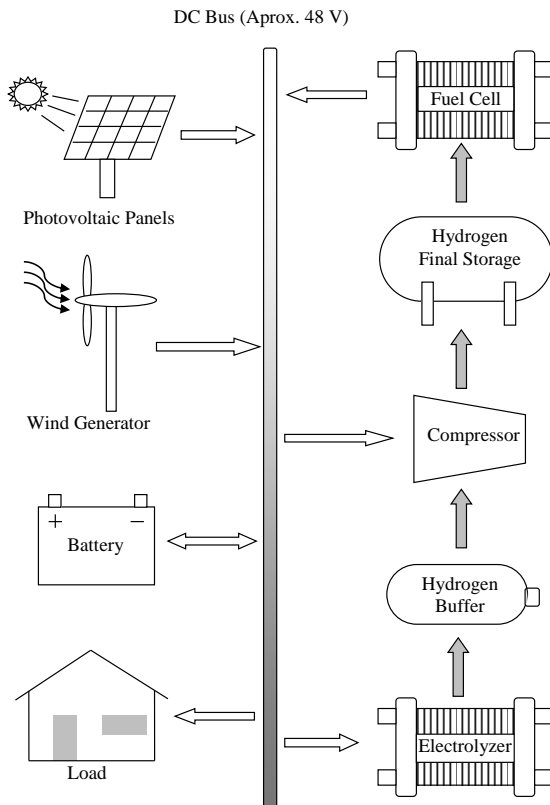

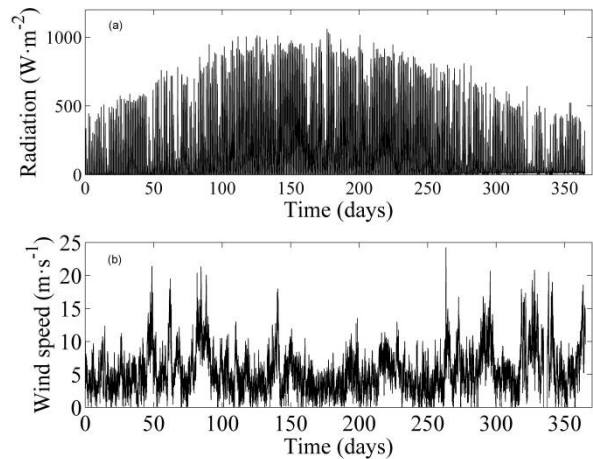Figure 1: Energy flows of general process scheme

Figure 2: Sunshine (a) and wind speed (b) data

means the wind energy source can step in to mitigate this reduction.

The demand curve was supplied by "Red Eléctrica de España", and in this case we have profiles for the average household on a typical day in summer and winter, with daily energy use taking into account the inverter of 8.55 kWh and 5.66 kWh, respectively. For fall and spring months an intermediate behavior, between the summer and winter profiles, is assumed (Fig. 3).
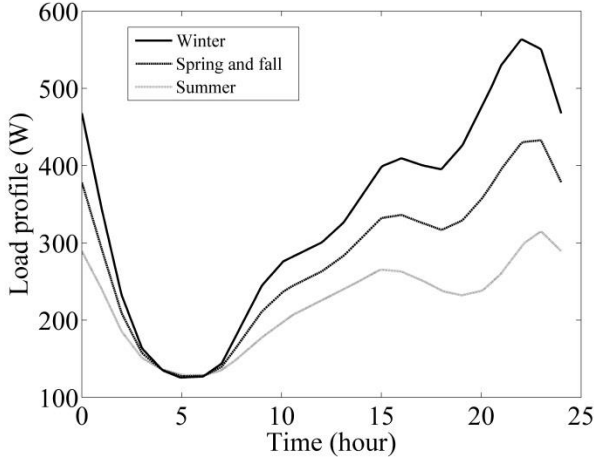

Figure 3: Load curve for a typical day in each season

2.2. Photovoltaic Panels

Radiation data are put into the block that calculates the energy supplied by each photovoltaic panel to the system. After passing through a previously created function, the power that a panel would be supplying is obtained according to room temperature and radiation being received in the case of following the maximum power curve, this curve will be calculated from the five parameter model presented by De Soto [18].

$$I_{pv} = I_L - I_0 \left[e^{\frac{V_{pv}+V_R}{a}} - 1 \right] - \frac{V_{pv} + I_{pv}R_S}{R_{Sh}} \tag{1}$$

Where V_{pv} (V) and I_{pv} (A) are the voltage and the current of the output, respectively, a (V^{-1}) is the ideality factor parameter, I_L (A) is the light current, I_0 (A) is the diode reverse saturation current, R_s (Ω) is the series resistance, and R_{Sh} (Ω) is the shunt resistance.

In this case (the photovoltaic panel shows a very high value in the parallel resistance) we can discard the third term on the right hand of the previous equation, reducing the equation to four parameters.

$$I_{pv} = I_L - I_0 \left[e^{\frac{V_{pv}+V_R}{a}} - 1 \right] \tag{2}$$

For data regarding the parameters used and how they are obtained from the technical specification of the photovoltaic module [19]. By multiplying the unitary power for each panel by the number of panels, 17 in this case, the power being generated by the panels at each moment is obtained. The main advantage of this model, apart from its reliability, accuracy and easy implementation, is the ease with which valid parameters are obtained in wide operation ranges from the data provided by the manufacturer, which in many cases are under standard nominal conditions, usually 1000 W/m² and 25 ℃.

2.3. Wind Generator

For simulation, wind speeds are put into the model block that refers to the wind generator in order to calculate the electrical energy produced by the device from the wind's kinetic energy. Each wind turbine has a characteristic curve that distinguishes it from the others, and defines the behavior it will have given various wind speeds, that is, it defines the power generated by the device for each wind value. The start up speed for the wind generator is approximately 3 m/s, which means that there is no energy output at wind speeds below this.

The wind generator model used is a Fortis Espada with 800 W of nominal power using two polyester reinforced, fiberglass blades with a 2.2 m rotor diameter. To determine the output power of the wind turbine in this case, we use a polynomial adjustment, [20] which relates wind speed to output power.

$$\left. \begin{array}{ll} P_{wt} = 0 & v < 3 \\ P_{wt} = 0.007(v-6)^2 + 0.06(v-6) + 0.13 & 3 \le v \le 8.5 \\ P_{wt} = -0.005(v-14)^2 + 0.04(v-14) + 0.068 & 8.5 \le v \le 20 \\ P_{wt} = 0.0008(v-22.4)^2 + 0.02(v-22.4) + 0.68 & 20 \le v \le 25 \\ P_{wt} = 0 & v > 25 \end{array} \right\} \tag{3}$$

Where P_{wt} is the output power of the wind generator (kW) and v is the wind speed (ms⁻¹).

2.4. Battery

Here, the battery fulfils three functions: firstly it is short-term storage for energy; secondly it provides the voltage for the DC bus; and thirdly it is used to provide one of the main energy management variables, which is the state of charge (SOC) of the battery, which will be explained later. In this case, the battery model and necessary parameters are provided by Agbossou et al. [21, 22]. Efficiency for battery operation is added to the model. In order to calculate voltage, we use:

$$U_{bat} = U_{bat,0} + R_{bat}I_{bat} \tag{4}$$

Where U_{bat} (V) is the voltage in the battery, $U_{bat,0}$ (V) is its voltage in open circuit, R_{bat} (Ω) is its internal resistance

and I_{bat} (A) is its current. If the sign of this last item is negative, then the battery is discharging, and if it is positive, it is charging. The total energy stored in the battery is:

$$E_B = E_{B,0} + \frac{1}{3600}\int I_B \eta_{bat} dt \qquad (5)$$

Where $E_{B,0}$ (Ah) is the initial energy of the battery and η_{bat} is its efficiency, which is assumed at 0.85 for charging processes and 1 for discharging processes. The SOC is given by:

$$SOC(\%) = 100\frac{E_B}{E_{B,\max}} \qquad (6)$$

Where $E_{B,max}$ (Ah) is the total capacity of the battery, enough to provide energy for between two and three days in winter.

2.5. Electrolyzer

In the electrolyzer, the current passes through a series of electrolytic cells in which there is a water input current that, due to the electrolysis provoked by the electric current, is split into two separate currents of hydrogen and oxygen.

The current-voltage curve chosen for the electrolyzer is that proposed by Satarelli et al.[5] for a bipolar 1 kW nominal power electrolyzer with 20 cells, operating at 80º and with Faraday efficiency assumed at 99%. In these simulations two electrolyzers are used.

The number of active electrolyzers depends on the input power, when this exceeds 1 kW nominal for one electrolyzer, then both of them are switched on. The characteristic curve to describe electrolyzer cell behavior is given by the following equation:

$$V_e = V_{e,0} + b\ln\left(\frac{I_e}{I_{e,0}}\right) + R_e I_e \qquad (7)$$

Where V_e (V) is the voltage of a cell, $V_{e,0}$ (V) is the reversible voltage for a cell, b (V^{-1}) is a characteristic coefficient of the electrolyzer, $I_{e,0}$ (A) is the exchange current, R_e (Ω) is the Ohmic resistance in the cell and I_e (A) is the current.

The electrolyzer only functions at powers of over 15% its nominal power. A parasitic loss of 50 W is assumed for each electrolyzer switched on

2.6. Compressor Buffer

The compressor buffer is an intermediate tank between the gas outlet from the electrolyzer, which works continually, and the compressor input. The second function it has is as a control system for the tank level, which, on reaching a set level activates an emptying signal to the compressor to evacuate the hydrogen towards the higher capacity tank.

The two input variables are the electrolyzer output flow and the flow to the compressor creating a hydrogen balance that, by being integrated, represents the amount of hydrogen.

$$\frac{dN_{H_2,Buf}}{dt} = F_{H_2,Buf,in} - F_{H_2,Buf,out} \qquad (8)$$

Where $N_{H2,Buf}$ is the number of accumulated moles in the buffer, $F_{H2,Buf,in}$ ($mols^{-1}$) the hydrogen flow entering from the electrolyzer and $F_{H2,Buf,out}$ ($mols^{-1}$) the output towards the compressor.

Applying a logical comparison system with memory, a trigger signal can be sent once a particular level is reached and a deactivation signal can be sent if a lower level is reached. Here, the trigger is at 95% of tank capacity and deactivation is at 40%. The buffer holds 1000 liters.

2.7. Compressor

When the buffer reaches the desired level, the compressor is triggered and compresses the hydrogen at 300 W, to achieve a lower volume of gas and thus a smaller final storage tank. A discontinuous flow model has been chosen, to avoid large hydrogen flows to the compressor that would need a much more powerful compressor. In this case, final storage pressure is 20 bar, the initial one being given by the buffer pressure, and compression takes place in three stages in such a way that the amount of hydrogen compressed is at a maximum, which is achieved when the ratio between the output and input pressures for each compressor stage are equal.

The molar flow of compressed hydrogen is equal to:

$$F_{H_2,comp} = P_{et,comp}\frac{n_{poly}-1}{n_{poly}}\eta_{comp}\frac{\eta_{comp}}{RT\left[\left(\frac{P_2}{P_1}\right)^{\frac{n_{poly}-1}{\eta_{poly}}}-1\right]} \qquad (9)$$

n_{poly} is the polytropic coefficient, in this case 1.36, η_{comp} is the efficiency of the compression with a value of 0.77, P_1 (bar) and P_2 (bar) the input and output pressures, respectively, $P_{et,comp}$ is the energy used in a stage, in this case 100 W, due to the fact that the output and input pressures are equal and therefore the energy consumed at each stage is equal.

2.8. Final Storage Tank

The tank is the final element in the model. The tank model is simple, here the inflow from the compressor and outflow to the fuel cell of hydrogen is taken into account at all in times and this is integrated order to have a real value for the amount of hydrogen stored throughout the year.

Thus, using the evolution of the amount of hydrogen, the tank can be scaled accordingly, and this is covered in the results section. The balance for the tank is the following

$$\frac{dN_{H_2,Tank}}{dt} = F_{H_2,in,Tank} - F_{H_2,out,Tank} \qquad (10)$$

Where: $dN_{H2,Tank}$ is the number of accumulated moles, $F_{H2,out,Tank}$ (mols^{-1}) the hydrogen flow entering from the compressor and $F_{H2,Tank}$,out (mols^{-1}) the output towards the fuel cell.

2.9. Fuel Cell

The fuel cell works in the opposite way to the electrolyzer, thus unregulated direct electrical current and water are obtained from the combination of hydrogen and oxygen. The input current at the anode will be the hydrogen obtained by means of electrolysis, supplied by the pressurized storage tank, whereas the input current at the cathode will be air with approximately 21% oxygen, reacting gas, and nitrogen, which is inert.

The cell we use in the model is the Nexa^{TM} by Ballard. In this particular case, to simulate the behavior of this element, we will use data supplied by the manufacturer, [23,24] which provides more than acceptable precision for the simulation we aim to carry out. Obtaining operational values for the cell through polynomial adjustments is relatively straightforward.

$$P_{fc,total} = 0.1755I_{fc,net}^2 + 40.218I_{fc,net} + 33.214 \qquad (11)$$

$$P_{fc,total} = -0.2247I_{fc,net}^2 + 37.46I_{fc,net} - 8.8164 \qquad (12)$$

$$P_{fc,total} = 0.0033I_{fc,net}^3 - 0.1807I_{fc,net}^2 + 6.765I_{fc,net} - 30.158 \qquad (13)$$

$$V_{fc,H_2} = 0.3832I_{fc.net} + 0.0419 \qquad (14)$$

Where $P_{fc,total}$ (W) is the total power of the cell, $P_{fc,net}$ (W) is the output power of the cell, $P_{fc,para}$ (W) is the parasitic loss of power through auxiliary equipment operation, $V_{fc,H2}$ (SLPM/s) is the flow of total hydrogen liters in standard conditions used by the cell and $I_{fc,net}$ (A) is the output current produced by the cell.

2.10. Energy Control and Management

What should first be borne in mind when choosing a suitable control system is that best energy use occurs when it is sent directly to meet load demands, next best is when it passes through the battery and lastly when hydrogen transformation takes place. 4

The variables used in controlling and managing energy are demand, energy entering and leaving the system, SOC, and the operational states of the fuel cell and the electrolyzer (0 and 1, on and off, respectively).

Together with these variables, three points are marked (EL = 85, FC$_{up}$ = 50 y FC$_{down}$ = 40) [18] that limit the four areas (Fig. 4) [19] where the SOC can be found and thus the areas of actuation for the operation of the battery, of the cell and of the electrolyzer are marked.

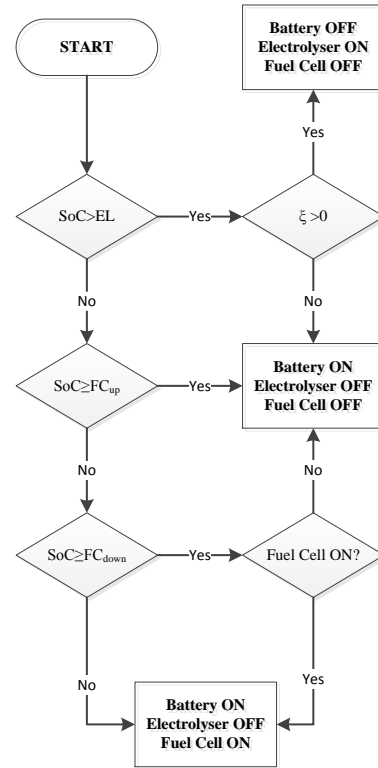The energy to be managed between the above units is defined as:

Figure 4: Control process scheme

$$f = P_{sun} + P_{wind} + P_{fc} - P_{load} - P_{comp} \qquad (15)$$

Where f (W) is the energy left over once demand is met, P_{sun} (W) is the power supplied by the photovoltaic panels, P_{wind} (W) is the power supplied by the wind generator, P_{fc} (W) is the power provided by the fuel cell, P_{load} (W) is the load demand and P_{comp} (W) the demand from the compressor. When f = 0, the energy accumulated by the system is zero, leftover energy is managed by the battery and the electrolyzer, whilst the deficits are managed by the fuel cell and the battery. In this case the electrolyzer and the battery work at variable power, depending on the requirements of the system, while the fuel cell always operates at fixed power. Below we comment on each of the zones:

Zone 1 (SOC > EL): only the battery and the electrolyzer operate, but they do so is an exclusive way. Thus, if f < 0, when there is an energy shortfall, the battery operates, and when f > 0, then the electrolyzer operates due to the energy excess. Zone 2 (EL$_{down}$ ≥ SOC ≥ FC$_{up}$): only the battery operates. Zone 3 (FC$_{up}$ > SOC > FC$_{down}$): only the battery and the fuel cell operate, but they do so in a nonexclusive way. The battery always works except when f = 0, and the fuel cell, unlike the electrolyzer, gives a set power. In this zone the only requirement for fuel cell operation is that it continues to function if it was doing so in the previous time step. Zone 4 (SOC <FC$_{down}$): Here, the battery and the fuel cell operate in a nonexclusive way. Thus for SOC values lower than FC$_{down}$ the fuel cell always operates.

3. Results and discussion

Renewable energies provide the system with 3819.7 kWh. Of this energy supply, 1167.6 kWh are due to wind energy and 2652.2 kWh to solar energy.

Fig. 5 shows the energy provided by each of these energy sources. For wind most energy is supplied at the start and end of the year, whereas the energy produced by the photovoltaic panels is concentrated around the center months of the year.

Load consumption is 2587.9 kWh, for hydrogen compressor is 33.6 kWh. In Fig. 6 the use of energy can be seen; this is distributed equally along the three routes open to it: 1438.6 kWh (38%) go straight to the load, 1196.1 kWh (31%) go to the battery, and 1185.1 kWh (31%) go to the electrolyzer. Fig. 6 is useful for getting a general idea of the energy distribution, but a clearer picture showing the operation of the various units in meeting load coverage throughout the year might perhaps be better seen in charts showing the evolution of accumulated energy throughout the year for the battery, and the input and output flows in the case of the fuel cell and the electrolyzer.

The battery remains charged to a maximum level (Fig. 7) during the central months of the year, which means that excess energy is sent to the electrolyzer for hydrogen production (Fig. 8a).
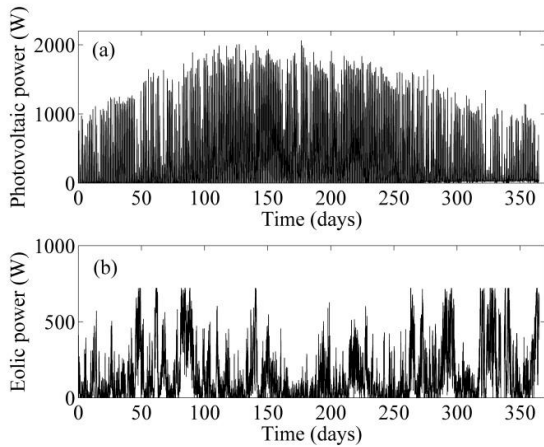

Figure 5: Power supplied by solar panels (a) and wind generator (b) to the system
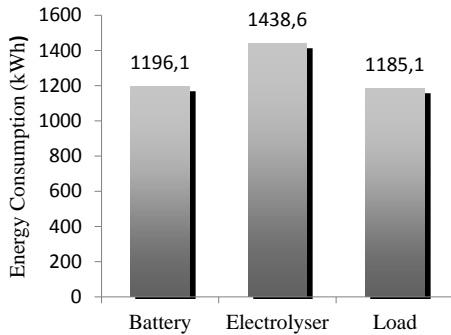

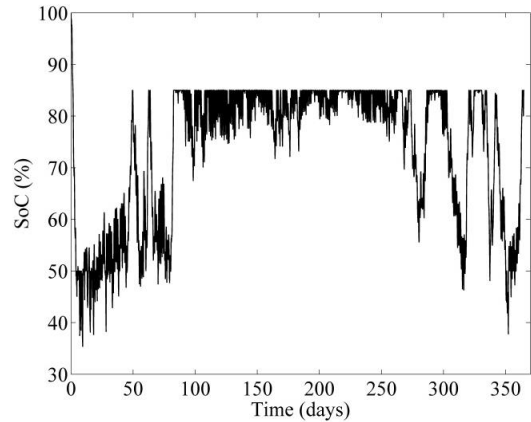Figure 6: Use of the energy that reaches the process from renewable sources

Figure 7: Energy supplied to the electrolyzer (a) and supplied by the fuel cell (b) over time

This is because the combination of the renewable energy sources at this period results in a high level of energy production. During this season peaks of over 1500 W from photovoltaic source appear, and to this must be added a respectable amount from the wind source, even though this is its low season.

At both ends of the year, we find zones where the fuel cell becomes operational (particularly at the start of the year) (Fig. 8b), because, despite wind energy showing production peaks due to the strong currents typical of the period, this is not enough to meet demand as solar production does not provide the same amount as in the central months. Thus we find that demand at the beginning and end of the year can be met by hydrogen produced in the middle months.

Finally we deal with the size of the hydrogen storage tank, for which it is helpful to understand the evolution of the amount of hydrogen stored over the year. This can be seen in Fig. 9; here the quantity of moles accumulated throughout the year is shown, not only for 17 solar panel system, with which the simulation was carried out, but also for 14 and 18 panels, in order to study other possibilities.

The aim when producing these charts was to obtain a positive yearend balance for the number of accumulated
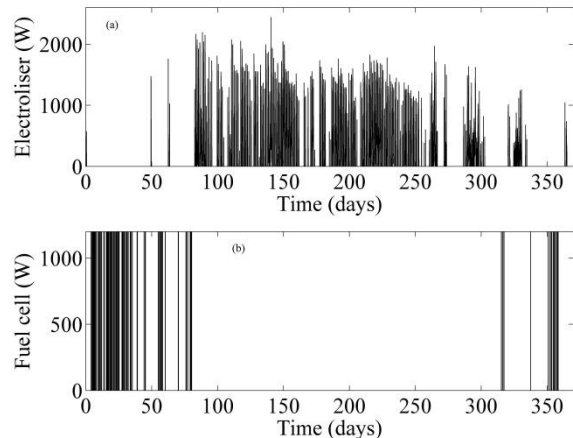

Figure 8: Energy supplied to the electrolyzer (a) and supplied by the fuel cell (b) over time
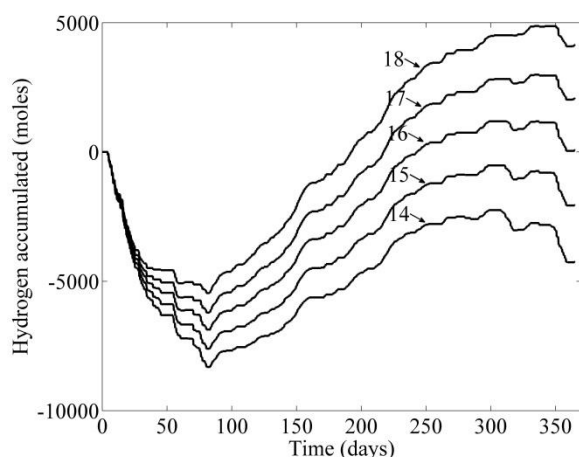
Figure 9: Evolution of the quantity of H_2 accumulated throughout the year for 14 – 18 photovoltaic panels

moles, so as to have a self-sufficient system. If this were not the case, resort would have to be made to an external energy source.

With regard to cases with 14 and 15 parameters, it can be seen that they are not self-sufficient; the one with 16 only just achieves this criterion, which means that at certain times during the year problems could arise in maintaining the pressure needed in the tank to supply hydrogen to the fuel cell. With 17 and 18 parameters, the balance is positive but 17 are favored because it requires less volume in the tank.

It can be seen that a demand for hydrogen is produced during the first months of the year and thus these are the months when there is highest consumption of hydrogen, coinciding with reduced renewable energy production. Almost all the hydrogen is produced during the middle months, when most of the annual energy overcapacity is also produced. In the final months of the year we find a balanced state followed by a drop, due to similarity between energy production and demand which then alters when energy production decreases and the balance is lost.

Thus an 11 m^3 tank is necessary for 20 bar. The time of installation is also important as the initial amount of hydrogen or, lacking that, energy from an external source, must be known.

4. Conclusions

In this work we have presented a model and its simulation for supplying a load demand by means of renewable energy sources (wind and solar), with batteries and hydrogen as short- and long-term energy reserves, respectively. The hydrogen is produced by means of an electrolyzer, compressed, stored and then converted to energy by a fuel cell when necessary.

The model consists of a series of units that function in steady state, and which were implemented in a dynamic global simulation. Using a control system, energy was managed and distributed between several possibilities: 38% direct to the load 31% to the battery, and 31% to the electrolyzer. Due to meteorological conditions, hydrogen is

accumulated in the middle months of the year, when the short-term, battery storage is enough to meet demand. Finally, using the evolution of the amount of accumulated hydrogen we estimated a storage tank size of 11 m^3. In this way the simulation of hybrid systems becomes a powerful tool for calculating and dimensioning the equipment involved, and thus a clear idea of the requirements for later construction is gained.

References

[1] Goldemberg, J., Ethanol for a Sustainable Energy Future Science , 315, pp. 808-810, 2007.

[2] Moriarty, P., Honnery D., What Energy Levels can the Earth Sustain?, Energy Policy, 37, pp. 2469-2474, 2009.

[3] Kannan, K. S., Strategies for Promotion and Development of Renewable Energy in Malaysia, Renewable Energy, 16, pp.1231-1236, 1999.

[4] Jacobsson, S., Lauber V., The Politics and Policy of Energy System Transformation - Explaining the German Diffusion of Renewable Energy Technology, Energy Policy , 34, pp. 256-276, 2006.

[5] Santarelli, M., Call, M., Macagno, S., Design and Analysis of Stand-Alone Hydrogen Energy Systems with Different Renewable Sources, Int J Hydrogen Energy, 29, pp. 1571-1586, 2004.

[6] Kolhe, M., Agbossou, K., Hamelin, J., Bose, T. K., Analytical Model for Predicting the Performance of Photovoltaic Array Coupled with a Wind Turbine in a Stand-Alone Renewable Energy System Based on Hydrogen, Renewable Energy, 28, pp. 727-742, 2003.

[7] Greiner, C. J., KorpÅs, M., Holen A. T., A Norwegian Case Study on the Production of Hydrogen from Wind Power, Int J Hydrogen Energy, 32, pp. 1500-1507, 2007.

[8] Vidueira, J. M., Contreras, A., Veziroglu, T. N., PV Autonomous Installation to Produce Hydrogen Via Electrolysis and its use in FC Buses, Int J Hydrogen Energy , 28, pp. 927-937, 2003.

[9] Chedid, R., Akiki, H., Rahman, S., A Decision Support Technique for the Design of Hybrid Solar-Wind Power Systems, IEEE Trans Energy Convers, 13, pp. 76-83, 1998.

[10] Hollmuller, P., Joubert, J., Lachal, B., Yvon, K., Evaluation of a 5 kWp Photovoltaic Hydrogen Production and Storage Installation for a Residential Home in Switzerland, Int J Hydrogen Energy, 25, pp. 97-109, 2000.

[11] Obara, S., Power Characteristics of a Fuel Cell Micro-Grid with Wind Power Generation, Int J Energy Res , 31, pp. 1064-1075, 2007.

[12] Lenzen, M., Wachsmann, U., Wind Turbines in Brazil and Germany: An Example of Geographical Variability in Life-Cycle Assessment, Appl Energy, 77, pp. 119-130, 2004.

[13] Realpe, A., Diazgranados, J.A., Acevedo, M.T., Electricity Generation and Wind Potential Assessment in Regions of Colombia, DYNA, 171, pp. 116-122, 2012.

[14] Ringel, M., Fostering the use of Renewable Energies in the European Union: The Race between Feed-in Tariffs and Green Certificates, Renewable Energy, 31, pp. 1-17, 2006.

[15] Lloyd, B., Subbarao, S., Development Challenges Under the Clean Development Mechanism (CDM) — Can Renewable Energy Initiatives be Put in Place before Peak Oil?, Energy Policy, 37, pp. 237-245, 2009.

[16] Busby, R.L., Hydrogen and Fuel Cells: a Comprehensive Guide, Tulsa: PennWell Corporation; 2005.

[17] Xunta de Galicia, Meteogalicia (Xunta de Galicia). Available at: http://www.meteogalicia.es [Accessed December 2013].

[18] De Soto, W., Improvement and Validation of a Model for Photovoltaic Array Performance, [PhD Thesis], 2004.

[19] Ai, B., Yang, H., Shen, H., Liao, X., Computer-Aided Design of PV/Wind Hybrid System, Renewable Energy , 28, pp. 1491-1512, 2003.

[20] Bilodeau, A., Agbossou, K., Control Analysis of Renewable Energy System with Hydrogen Storage for Residential Applications, J Power Sources, 162, pp. 757-764, 2006.

[21] Kélouwani, S., Agbossou, K., Chahine, R., Model for Energy Conversion in Renewable Energy System with Hydrogen Storage, J Power Sources, 140, pp. 392-399, 2005.

[22] Ballard Power Systems Inc., Nexa Power Module User's Manual, 2003.

[23] Zhou, K., Ferreira, J.A., de Haan, S.W.H., Optimal Energy Management Strategy and System Sizing Method for Stand-Alone Photovoltaic-Hydrogen Systems, Int J Hydrogen Energy, 33, pp. 477-489, 2008.

[24] Ulleberg, O., The Importance of Control Strategies in PV-Hydrogen Systems, Solar Energy, 76, pp. 323-329, 2004.